Draft version May 5, 2025
Typeset using LaTeX **twocolumn** style in AASTeX7

Stellar Structure Report Spring 2025

Hayley Nofi[1]

[1] *Johns Hopkins University*

ABSTRACT

We present a stellar structure model of a 1.4 $M_\odot$ zero age main sequence star (ZAMS) with X = 0.7, Y = 0.28, and Z = 0.02. The model is numerically calculated by solving the coupled differential equations of stellar structure via shooting and integration from an inner boundary and an outer boundary. The inner boundary is located closer to the center of the star. The outer boundary is located at the star's photosphere, where the optical depth is 2/3. We assume the star is in hydrostatic equilibrium, chemical homogeneity, and the star is non-rotating. The energy transport is either radiative or adiabatic for solving for the pressure. The energy generation is solved using the proton-proton chain and CNO cycle energy only. The opacity is interpolated using a table from the Los Alamos National Laboratory (N. Magee et al. 1995). The result from the stellar structure model is compared to the MESA output for a star with identical mass and composition. The model agrees with MESA predictions to within 10–25% for stellar parameters such as luminosity, radius, pressure, and temperature. Discrepancies are discussed in terms of boundary conditions, convergence behavior, and physics simplifications.

1. INTRODUCTION

Zero age main sequence (ZAMS) is defined as when the nuclear reactions begin in a star and generate luminosity.The "zero-age" refers to how the star has had very little change in luminosity, radius, and effective temperature since it first started hydrogen fusion. This phase can last for a few thousand years for a massive star, 10^7 years for a solar mass star, and 10^9 for the least massive stars (C. J. Hansen & S. D. Kawaler 1994). ZAMS stars fall on the edge of the main sequence branch on the HR diagram.

Understanding the internal structure of stars is important for stellar astrophysics. ZAMS stars are the ideal candidate to model because you do not have to worry about prior evolution history as hydrogen just began to burn. By solving the four fundamental differential equations of stellar structure—mass conservation, hydrostatic equilibrium, energy transport, and energy generation—we can construct models that describe how pressure, temperature, luminosity, and radius vary with depth. In this project, we numerically solve these equations for a 1.4 $M_\odot$ ZAMS star. We compare our results with results for a star with the same mass using Modules for Experiments in Stellar Astrophysics (MESA), an advanced, open-source 1D stellar evolution code (B. Paxton et al. 2011).

In Section 2 we introduce the model criteria. In Section 3 we describe our boundary conditions conditions imposed on the stellar center and surface. In section 4 we describe the overall approach for converging on the best model. In section 5 we present the results from our model, a machine-readable table of the model output, and the MESA output. In section 6 we discuss the discrepancies between the our model and the MESA output. In section 7 we present our conclusions.

2. MODEL DESCRIPTION

We model a 1.4 $M_\odot$ zero age main sequence star (ZAMS) in hydrostatic equilibrium. The star is chemically homogeneous with a hydrogen mass fraction of X = 0.7, helium mass fraction of Y = 0.28, and metal mass fraction of Z = 0.02. The opacity for the model is interpolated from a table from the Los Alamos National Laboratory (N. Magee et al. 1995) for the above elemental abundance using density and temperature.

The structure of a star in hydrostatic equilibrium is determined by the following four differential equations. In our model, the equations are expressed in terms of the enclosed mass coordinate m rather than radius r (C. J. Hansen & S. D. Kawaler 1994):

1. **Luminosity Gradient**

$$\frac{dL}{dM_r} = \epsilon \tag{1}$$

2. **Hydrostatic Equilibrium**

$$\frac{dP}{dM_r} = -\frac{Gm}{4\pi r^4} \tag{2}$$

3. **Radius Gradient**

$$\frac{dr}{dM_r} = \frac{1}{4\pi r^2 \rho} \tag{3}$$

4. **Temperature Gradient**

$$\frac{dT}{dM_r} = -\frac{GmT}{4\pi r^4 P}\nabla \tag{4}$$

Where M_r is the Lagrangian mass coordinate, ϵ is the the energy generation rate per unit mass, r is the radius, ρ is the density, T is the temperature, and ∇ is the logarithmic gradient. The model uses CGS units throughout. The Lagrangian mass coordinate M_r is defined as:

$$M_r = \int_0^r 4\pi r^2 \rho dr \tag{5}$$

The logarithmic gradient ∇ is defined as:

$$\nabla = \frac{d\ln(T)}{dln(P)} \tag{6}$$

The radiative temperature gradient $\nabla_{\rm rad}$ is given by:

$$\nabla_{rad} = \frac{3}{16\pi acG}\frac{P\kappa}{T^4}\frac{L_r}{M_r} \tag{7}$$

The adiabatic temperature gradient $\nabla_{\rm ad}$ is given by:

$$\nabla_{ad} = \frac{2(4-3\frac{P_{gas}}{P_{gas}+P_{ad}})}{32-24\frac{P_{gas}}{P_{gas}+P_{ad}} - 3\frac{P_{gas}}{P_{gas}+P_{ad}}^2} \tag{8}$$

The choice of whether the temperature gradient is radiative or adiabatic is determined by comparing $\nabla_{\rm rad}$ and $\nabla_{\rm ad}$:

$$\nabla = \nabla_{rad} \text{if} \nabla_{rad} < \nabla_{ad} \tag{9}$$

$$\nabla = \nabla_{ad} \text{if} \nabla_{rad} > \nabla_{ad} \tag{10}$$

Another important piece of the stellar structure calculation is the equation of state. If we assume the star's gas and radiation are in a state of local thermodynamic equilibrium, the equation of state can be given by the ideal gas law and radiation pressure:

$$P = P_{gas} + P_{rad} = \frac{\rho N_A kT}{\mu} + \frac{aT^4}{3} \tag{11}$$

Energy generation for the ZAMS star is assumed to be due to the proton-proton (PP) chain and CNO cycle only. The energy generation rate for the PP chain is given by:

$$\epsilon_{PP} = 2.57\times10^4 \psi f_{11} g_{11} \rho X^2 T_9^{-2/3} e^{-3.381/T_9^{1/3}} \tag{12}$$

The function g_{11} is:

$$g_{11} = 1 + 3.82T_9 + 1.51T_9^2 + 0.144T_9^3 - 0.0114T_9^4 \tag{13}$$

Where ψ is a factor dependent on the temperature, and f_{11} is a factor that is set to 1 for simplicity.

The energy generation rate for the CNO cycle is given by:

$$\epsilon_{CNO} = 8.24\times10^25 g_{141} X_{CNO} X \rho T_9^{-2/3} e^{-15.231T_9^{-1/3} - (T_9/0.8)^2} \tag{14}$$

The function g_{141} is:

$$g_{141} = 1 - 2.00T_9 + 3.41T_9^2 - 2.43T_9^3 \tag{15}$$

We assume $X_{\rm CNO} = Z$, with metals being mostly carbon, oxygen, and nitrogen.

3. BOUNDARY CONDITIONS

At the core, we apply the following boundary conditions (R. Kippenhahn et al. 2013):

1. **Luminosity at core**

$$L_c = (\epsilon_{PP} + \epsilon_{CNO}) \cdot M \tag{16}$$

2. **Pressure at core**

$$P_c = P - \frac{3G}{8\pi}\left(\frac{4\pi}{3}\rho\right)^{4/3} \cdot M^{2/3} \tag{17}$$

3. **Radius at core**

$$R_c = \frac{3M}{4\pi\rho_c}^{1/3} \tag{18}$$

4. **Temperature at core**

$$T_c = \left(T^4 - \frac{1}{2ac}\frac{3}{4\pi}^{2/3}\kappa(\epsilon_{PP} + \epsilon_{CNO})\rho_c^{4/3} M^{2/3}\right)^{1/4} \tag{19}$$

At the surface, we impose the total radius and luminosity and use the Stefan-Boltzmann law to estimate the surface temperature. The surface pressure is approximated using (R. Kippenhahn et al. 2013):

1. **Luminosity at surface**

$$L_s = L \tag{20}$$

2. **Pressure at surface**

$$P_s = P - \frac{3G}{8\pi}\left(\frac{4\pi}{3}\rho\right)^{4/3} \cdot M^{2/3} \tag{21}$$

3. **Radius at surface**

$$R_s = R \tag{22}$$

4. **Temperature at surface**

$$T_s = T_{eff} = \left(\frac{L}{4\pi R^2 \sigma}\right)^{1/4} \tag{23}$$

Luminosity [ergs/s]	1.2×10^{34}
Pressure [dyne/cm^2]	2×10^{17}
Radius [cm]	7×10^{10}
Temperature [K]	1.75×10^{7}

Table 1. Initial conditions

4. NUMERICAL METHODS

The stellar structure equations (equations 1-4) are integrated from both the center and the surface following the boundary conditions defined in 3 using the Runge-Kutta method (RK45) implemented in scipy.integrate.solve_ivp (P. Virtanen et al. 2020). We use the shooting method to converge on the set of stellar parameters that best satisfy our boundary conditions. The shooting method is a numerical technique for solving boundary value problems by converting them into a series of initial value problems. It works by guessing initial conditions at one boundary, integrating the system of differential equations to the other boundary, and then adjusting the guess to minimize discrepancies with the target boundary conditions. The "pure" shooting method integrates from one end to the other, while the "shooting to a fitting point" integrates from both ends toward an intermediate point attempting to match conditions at the midpoint (W. H. Press et al. 1992). Our process uses the "shooting to a fitting point" procedure. The initial conditions chosen were based on the values from the MESA mode of the identical star and are shown in Table 1.

We also develop a function to repeatedly call a our shooting function, calculate updated boundary values, and obtain a converged solution. For this we use globally convergent Newton method. This method combines the rapid local convergence of Newton's method with a higher-level strategy that guarantees either progresses toward an actual root or toward failure to converge. The algorithm first computes a Newton step direction δx from the Jacobian J, then performs a backtracking line search along that direction to find a step length λ that reduces a scalar merit function sufficiently. This guarantees that the method always makes progress, even if the initial Newton step is poor (W. H. Press et al. 1992). This is implemented using scipy.optimize.minimize and setting the method to 'Newton-CG' (P. Virtanen et al. 2020).

5. RESULTS

The results from our stellar structure model are presented in figures showing the convergence of luminosity, pressure, radius, and temperature from the center of the star to the surface. The convergence for the initial conditions is shown in Figure 1. This figure shows the evolution of these physical quantities as we solve the stellar structure equations using the initial conditions provided by MESA. These initial conditions were taken from the MESA model for a star with identical mass and composition, as shown in Table 1.

Luminosity difference	20.76%
Pressure difference	7.51%
Radius difference	31.93%
Temperature difference	6.65%

Table 2. Percent difference between MESA and iterative stellar model values at core.

Next, we compare the results obtained by the initial condition approach to the iterative approach in Figure 2. In this approach, it took 7 iterations to converge. The method returned a warning: "Desired error not necessarily achieved due to precision loss," which suggests some numerical challenges at the boundary. However, despite the warning, the luminosity, pressure, and radius curves in this approach converge better than the initial conditions model.

Finally, in Figure 3, we compare the results from the iterative approach with the MESA output for a star with identical mass and composition. The luminosity curve from our model appears to follow the correct trend, but it is lower than the MESA luminosity. The pressure curve from our model is very close to the MESA result, and the radius curve is also quite close. However, the temperature curve from our model is consistently lower than the MESA temperature curve, indicating a discrepancy.

The percent error between the results of our model and MESA at the core is shown in Table 2. The luminosity difference is approximately 20.76%, the pressure difference is 7.50%, the radius difference is 31.93%, and the temperature difference is 6.64%. The radius percent error is relatively higher compared to the other parameters suggesting that the radius is not converging accurately.

Given these results, the model appears to agree reasonably well with MESA in terms of luminosity, pressure, and temperature, given the simplicity of the model. But there are discrepancies, particularly in radius. Potential reasons for the discrepancies between the stellar model and MESA are discussed in Section 6.

5.1. *Machine-readable output*

A full machine-readable table containing the variables M, L, P, R, T, ρ, ϵ, κ, ∇_{ad}, ∇, and convection state of the shell is available in the GitHub repository.

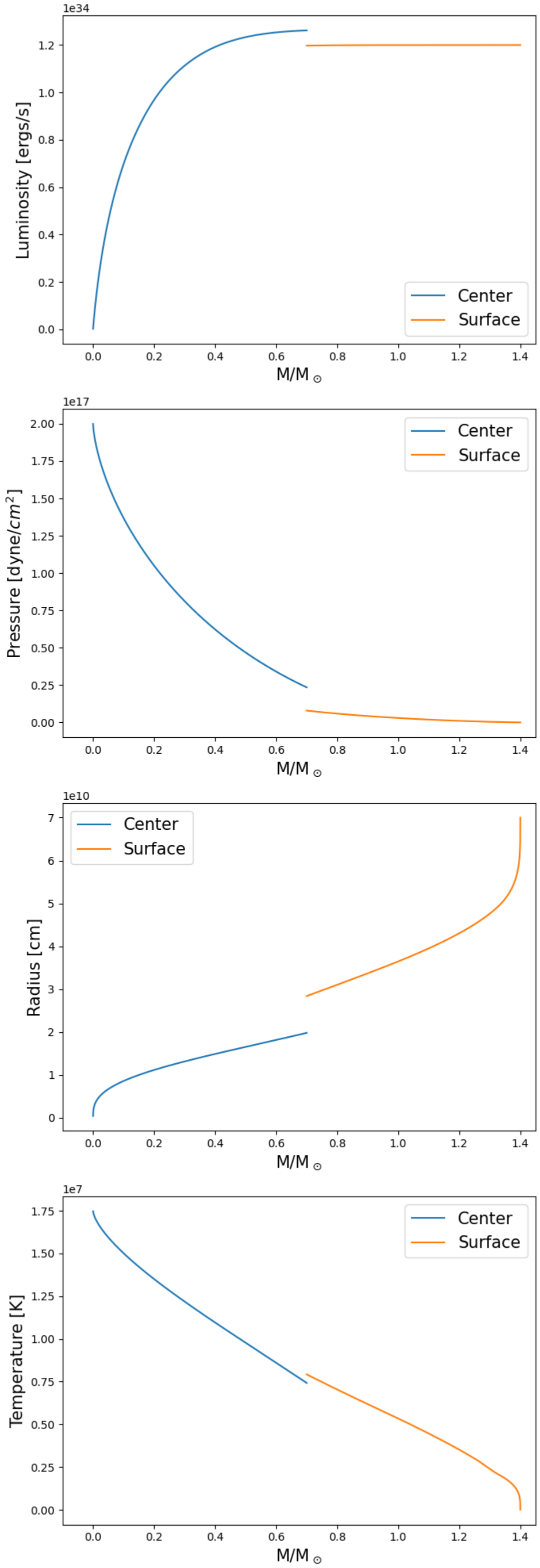

Figure 1. The result of the stellar structure code using initial conditions.

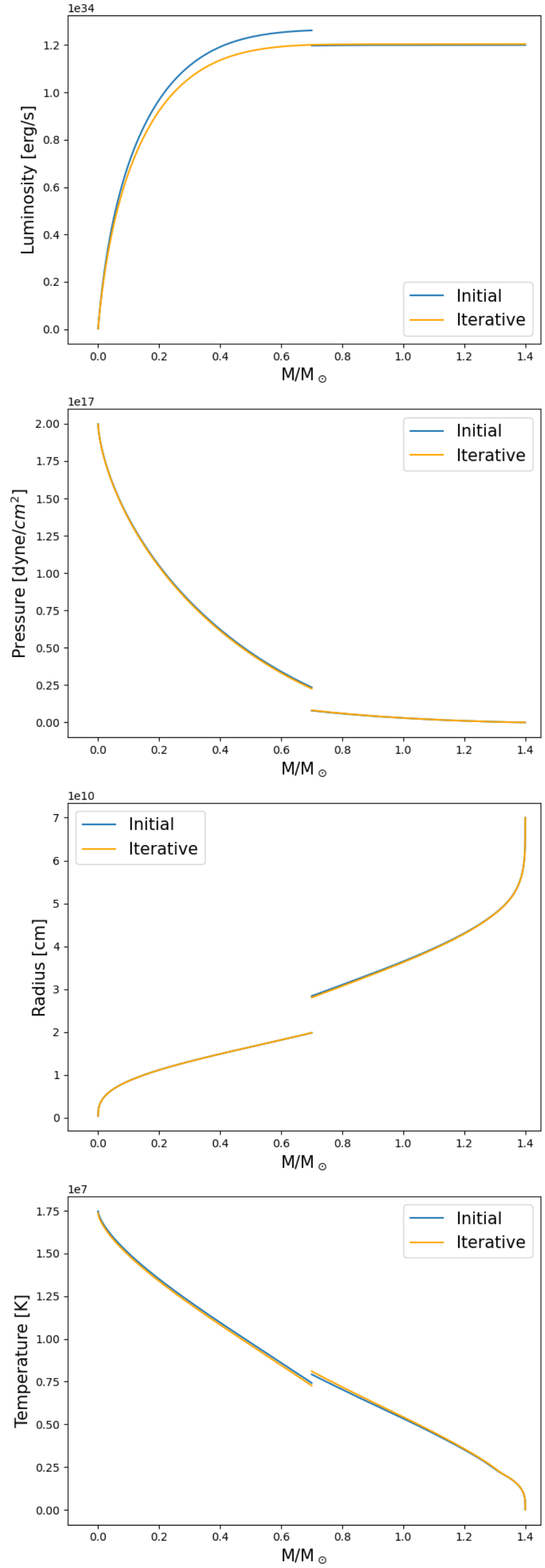

Figure 2. The result of the stellar structure code using initial conditions compared to the result of the stellar structure code using the iterative approach.

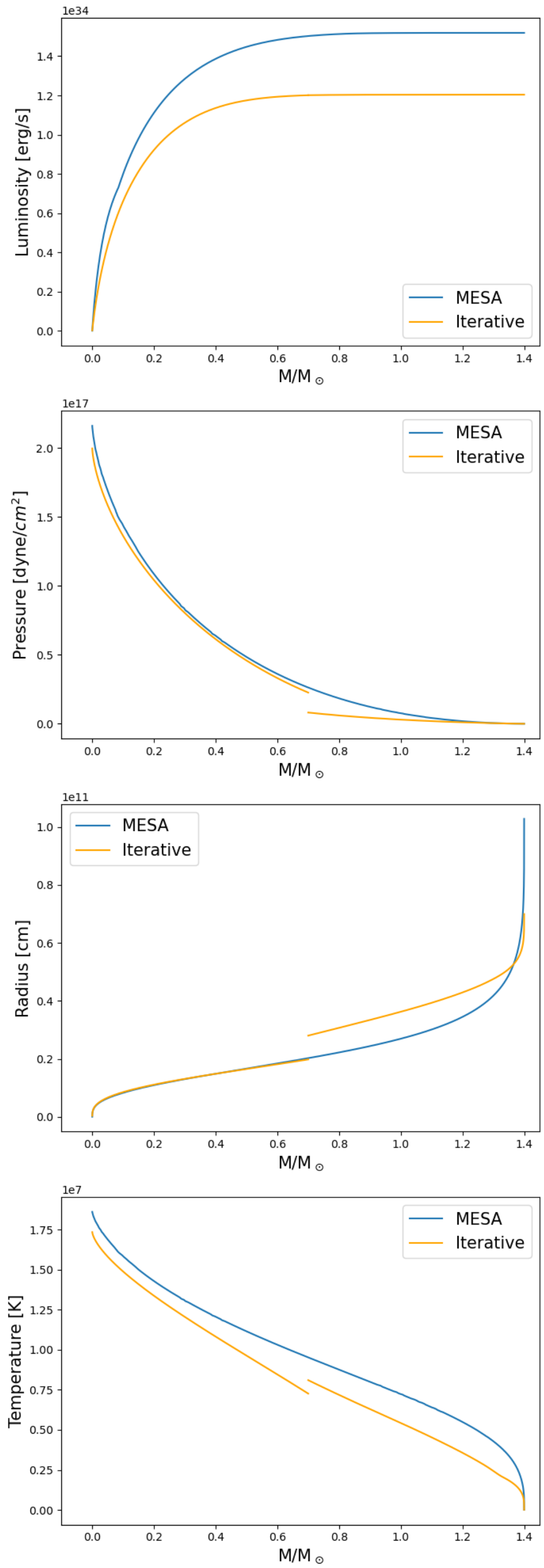

Figure 3. The result of the stellar structure code using the iterative approach compared to the output from MESA for a star with identical mass and composition.

6. DISCUSSION

The results presented in Section 5 reveal potential areas for improvement in our stellar structure model. While the model agrees reasonably well with MESA for luminosity, pressure, and temperature (with discrepancies mostly within the expected range of ≈5-20%), it does not perform as well for the radius. Several factors may contribute to these discrepancies:

1. **Initial Conditions:** The initial conditions were based on the MESA model. However, it may be more accurate to compute the initial luminosity, pressure, radius, and temperature using numerical expressions.

2. **Convergence Issues:** We experienced issues with the convergence of the globally convergent Newton method during the iterative fit. The high percent error for the radius may be the result of the method we used for solving the stellar structure equations may not be fully accurate in handling the radius equation, especially under the simplified conditions.

3. **Model Simplicity:** The model used in this paper is a simplified version compared to the one used in MESA. Therefore, we expect MESA to produce more accurate results due to their advanced treatment of physical processes ignored in our model.

7. CONCLUSIONS

We constructed a stellar model of a 1.4 $M_\odot$ main-sequence star. The model solves the stellar structure equations and incorporates realistic energy generation and opacity using opacity tables from the Los Alamos National Laboratory. While not as sophisticated as MESA, our model agrees with MESA to within ≈5–35% in luminosity, pressure, radius, and temperature.

GITHUB REPOSITORY

https://github.com/hnofi/AS.171.611-Final

REFERENCES

Hansen, C. J., & Kawaler, S. D. 1994, Stellar Interiors. Physical Principles, Structure, and Evolution., doi: 10.1007/978-1-4419-9110-2

Kippenhahn, R., Weigert, A., & Weiss, A. 2013, Stellar Structure and Evolution, doi: 10.1007/978-3-642-30304-3

Magee, N., Jr, A., Clark, R., et al. 1995, 78, 51

Paxton, B., Bildsten, L., Dotter, A., et al. 2011, ApJS, 192, 3, doi: 10.1088/0067-0049/192/1/3

Press, W. H., Teukolsky, S. A., Vetterling, W. T., & Flannery, B. P. 1992, Numerical recipes in FORTRAN. The art of scientific computing

Virtanen, P., Gommers, R., Oliphant, T. E., et al. 2020, Nature Methods, 17, 261, doi: 10.1038/s41592-019-0686-2